Modeling Uplink Coverage and Rate with Aggregation in Machine-to-Machine Communication Networks

Derya Malak, Harpreet S. Dhillon, and Jeffrey G. Andrews

***Abstract*—Machine-to-machine (M2M) communication's severe power limitations challenge the interconnectivity, access management, and reliable communication of data. In densely deployed M2M networks, coordinating and aggregating the generated data is critical. We propose an energy efficient data aggregation scheme for a hierarchical M2M network with truncated power control. We optimize the number of hierarchical stages and perform a coverage probability-based uplink analysis for M2M devices. Our analysis exposes the key tradeoffs between the coverage characteristics for successive and parallel transmission schemes that can be either half-duplex or full-duplex. Comparing the rate performances of the transmission models, we observe that successive and half-duplex parallel modes have better coverage characteristics compared to full-duplex parallel scheme.**

***Index Terms*—Machine-to-machine communication, aggregator, rate, coverage, uplink, truncated power control, network hierarchy, stochastic geometry.**

I. Introduction

Applications involving machine-to-machine (M2M) communication are rapidly growing, and will become an increasingly important source of traffic and revenue in current 4G and future 5G cellular networks. Unlike video applications, which are expected to consume around 70% of all wireless data by the end of the decade [1], M2M devices will use a comparatively smaller fraction. However, M2M communication has its own challenges. The air interface design for high-data-rate applications may not effectively support vast number of devices expected in M2M communications, each usually having only a small amount of data to transmit. Thus, M2M will require sophisticated access management and resource allocation with QoS constraints to prevent debilitating random access channel (RACH) congestion [2].

Unlike most human generated or consumed traffic, M2M as defined in this paper is characterized by a very large number of small transactions, often from battery powered devices. The power and energy optimal uplink design for various access strategies is studied in [3], while an optimal uncoordinated strategy to maximize the average throughput for a time-slotted RACH is developed in [4]. For the small payload sizes relevant for M2M, a strategy that transmits both identity and data over the RACH is shown to support significantly more devices compared to the conventional approach, where transmissions are scheduled after an initial random-access stage. An energy-efficient uplink design for LTE networks in M2M and human-to-human coexistence scenarios that satisfies QoS requirements is developed [5].

In M2M communication, critical design issues also include energy efficient data aggregation along with efficient hierarchical organization of the devices. Clustering is a key technique to reduce energy consumption and it increases the scalability and lifetime of the network [6]. Although these issues have not been studied in the context of M2M communication, there is prior work on distributed networks in the context of wired communications. In [7], energy consumption is optimized by studying a distributed protocol for stationary ad hoc networks. In [8], a distribution problem which consists of subscribers, distribution and concentration points for a wired network model is studied to minimize the cost by optimizing the density of distribution points. In [9], a hierarchical network including multiple sinks, aggregation nodes and sensors is proposed, which yields significant energy savings.

We propose an energy-efficient design for M2M uplink where devices have a maximum power constraint. Since the M2M devices are power limited and thus range limited, multi-hop routing is a feasible strategy rather than direct transmissions. However, in designing multi-hop protocols, the number of hops cannot be increased arbitrarily due to the additional energy consumption incurred by relays; long-hop routing is a competitive strategy for many networks [10]. Therefore, in this paper, we analyze a hierarchical M2M communication model with data aggregation involving multi-hop transmissions. Despite previous research efforts, e.g., [5], [11], to the best of our knowledge, there has been no study focusing on data aggregation schemes for M2M networks together with the rate coverage characteristics, especially from an energy optimal design perspective. Providing such a study is the main contribution of this paper.

We propose a general aggregator model for power limited M2M devices in Sect. II. Using stochastic geometry, we analyze the SIR and rate coverage characteristics of the multi-stage transmission process with truncated power control to determine the optimal number of stages (hops), which will be detailed in Sect. III. We consider two possible transmission techniques: i) *successive scheme*, where the hierarchical levels are not active simultaneously, and ii) *parallel scheme*, where either all the levels are active simultaneously as in full-duplex transmission or where the active levels are interleaved as in

D. Malak and J. G. Andrews are with the Wireless and Networking Communications Group (WNCG), The University of Texas at Austin, TX, USA. Email: deryamalak@utexas.edu, jandrews@ece.utexas.edu. H. S. Dhillon is with Wireless@VT, Department of Electrical and Computer Engineering, Virginia Tech, Blacksburg, VA, USA. Email: hdhillon@vt.edu.

Manuscript last revised: February 29, 2016.

half-duplex mode, which will be detailed in Sect. IV. In Sect. V, we provide a numerical performance comparison in terms of the communication rates of the proposed techniques.

II. Data Aggregation and Transmission Model

We consider a cellular-based uplink model for M2M communication where the BS and device locations are distributed as independent Poisson Point Processes (PPPs) with respective densities of $\lambda_{\rm BS}$ and λ with $\lambda \gg \lambda_{\rm BS}$. Devices transmit data to the BS by aggregation. The initial device process Ψ is independently thinned by probability $\gamma < 0.5$ to generate the aggregator process Ψ_a with density λ_a and the transmitter process Ψ_u with density λ_u, where $\lambda = \lambda_u + \lambda_a$. Each transmitter is associated to the closest aggregator, i.e., the transmitters in the Voronoi cell of the typical aggregator will transmit their payloads to that aggregator.

The aggregation process can be extended to multiple stages. Each hierarchical level is composed of the transmitter and the aggregator processes, where the aggregator processes of all stages are initially determined such that they are disjoint from each other. At each stage, after the set of transmitters transmit their payloads to their nearest aggregators, and once the transmissions of a hierarchical level are completed, the transmitters are turned off and excluded from the process. In the subsequent hierarchical level, the aggregators of the previous stage become the transmitters, and they transmit their data to the aggregator process of the new stage. The aggregation process is repeated over multiple stages to generate the hierarchical transmission model. The process ends when all the payload is transmitted to the BS in the last stage of this multi-hop process, which we call a transmission cycle.

The transmitter device density of the first stage is found by subtracting the total density of aggregators from the initial density of the device process as $\lambda_u(1) = \lambda - \sum_{k=1}^{K-1} \lambda_a(k)$. By the end of the first stage, the devices with a density of $\lambda_u(1)$ will transmit their payload to the aggregator process with a density of $\lambda_a(1)$. Next, at the second stage, the aggregators of the first stage form the new transmitting device process, i.e., $\lambda_u(2) = \lambda_a(1)$, and these devices transmit to the devices forming the set of second stage aggregator process with density $\lambda_a(2)$. The aggregation process can be extended to $k > 2$ stages in a similar manner by letting $\lambda_u(k) = \lambda_a(k-1)$ for $k \geq 2$. The important design parameters are tabulated in Table I, where $\bar{\gamma}_K = \sum_{k=1}^{K-1} \gamma^k$. In Fig. 1, we illustrate a three-stage model, where the aggregator process of stage k, i.e., $\Psi_a(k)$, is obtained by independently thinning Ψ with probability 0.4^k, i.e., $\Psi_a(k)$ has a density of $0.4^k\lambda$.

Each BS has an average coverage area of $\lambda_{\rm BS}^{-1}$, and each device has a fixed payload of M bits to be transmitted to the BS. We assume standard power law path loss model where the signal power decays as $d^{-\alpha}$ over distance d, where α is the path loss exponent. We also assume open loop power control with maximum transmit power constraint under which the transmit power of a device located at distance d from the BS is $P_T(d) = \min\{P_{T_{\max}}, \overline{P}_T d^{\alpha}\}$, where $P_{T_{\max}}$ is the maximum transmit power constraint and $\overline{P}_T$ is the received power when $d \leq \left(P_{T_{\max}}/\overline{P}_T\right)^{1/\alpha}$. With this assumption, the average received power at the BS from a device in its coverage area and located at distance d from the BS is constant and equal to $P_R(d) = \min\{P_{T_{\max}} d^{-\alpha}, \overline{P}_T\}$.

	$k=1$	$2 \leq k \leq K-1$	$k=K$
$\lambda_u(k)$	$\lambda(1-\bar{\gamma}_K)$	$\lambda\gamma^{k-1}$	$\lambda\gamma^{K-1}$
$\lambda_a(k)$	$\lambda\gamma$	$\lambda\gamma^{k}$	$\lambda_{\rm BS}$
$\mathbb{E}\left[\mathrm{N_a}(k)\right]$	$(1-\bar{\gamma}_K)/\gamma$	γ^{-1}	$\lambda\gamma^{K-1}/\lambda_{\rm BS}$
$\bar{t}_{\rm tx}(k)$	1	$(1-\bar{\gamma}_K)/\gamma^{k-1}$	$(1-\bar{\gamma}_K)/\gamma^{K-1}$

TABLE I: Design parameters.

III. SIR Coverage Probability

We propose a coverage-based model for data aggregation, assuming that the transmission is successful if the SIR of the device is above a threshold. We derive the coverage probability in the uplink for the proposed data aggregation model.

Orthogonal access is assumed in the uplink and at any given resource block, there is at most one device transmitting in each cell. Let Ψ_u be the process denoting the location of devices transmitting on the same resource as the typical device. The uplink SIR of the typical device $x \in \Psi_u$ located at distance $\|x\|$ from its aggregator on a given resource block is

$$\mathrm{SIR} = \frac{g \min\{P_{T_{\max}} \|x\|^{-\alpha}, \overline{P}_T\}}{\sum\limits_{z \in \Psi_u \setminus \{x\}} g_z \min\{P_{T_{\max}}, \overline{P}_T R_z^{\alpha}\} D_z^{-\alpha}}, \tag{1}$$

where R_z and D_z denote the distance between the transmitter aggregator pair and the distance between the interferer and the typical aggregator, respectively. The random variable $g_z \sim g$ is the small-scale iid fading parameter due to interferer z.

Assumption 1. *The actual distribution of R_z is very hard to characterize due to the randomness both in the area of the Voronoi cell of the aggregator and in the number of the devices it serves. Therefore, we approximate it by the distance of a randomly chosen point in $\mathbb{R}^2$ to its closest aggregator, i.e., by a Rayleigh distribution [12]:*

$$f_{R_z}(r_z) = (r_z/\sigma^2) e^{-r_z^2/2\sigma^2},\ r_z \geq 0,\ \sigma = \sqrt{1/(2\pi\lambda_a)}. \tag{2}$$

The uplink SIR coverage of the proposed system model with truncated power control is given by the following Lemma.

Lemma 1. The uplink SIR coverage with truncated power control: *With truncated power control and with minimum average path loss association[1], the uplink SIR coverage is*

$$\mathcal{P}(T) = p\mathcal{L}_{I_r}(T\overline{P}_T^{-1}) + \int_{r_c}^{\infty} \mathcal{L}_{I_r}(Tr^{\alpha}P_{T_{\max}}^{-1}) f_R(r)\,\mathrm{d}r, \tag{3}$$

where $p = 1 - \exp\left(-\pi\lambda_a r_c^2\right)$, R is Rayleigh distributed with parameter $\sigma = \sqrt{1/(2\pi\lambda_a)}$, and

$$\mathcal{L}_{I_r}(s) \approx e^{-\frac{2s}{\alpha-2}(1-e^{-\pi\lambda_a r_c^2}(1+\pi\lambda_a r_c^2))\overline{P}_T C_{\alpha}(s\overline{P}_T)} \\ e^{-\frac{2s}{\alpha-2}(1-p)\pi\lambda_a P_{T_{\max}} \mathbb{E}_{R_z}\left[R_z^{2-\alpha} C_{\alpha}(sP_{T_{\max}} R_z^{-\alpha}) \middle| R_z > r_c\right]} \tag{4}$$

denotes the Laplace transform of the interference where $C_{\alpha}(T) = {}_2F_1\left(1, 1-\frac{2}{\alpha}, 2-\frac{2}{\alpha}, -T\right)$, and ${}_2F_1$ is the Gauss-Hypergeometric function.

[1]In "minimum average path loss association", a device associates to an aggregator with minimum path loss averaged over the small-scale fading, i.e., the aggregator has minimum R_z^{α} product among all aggregators.

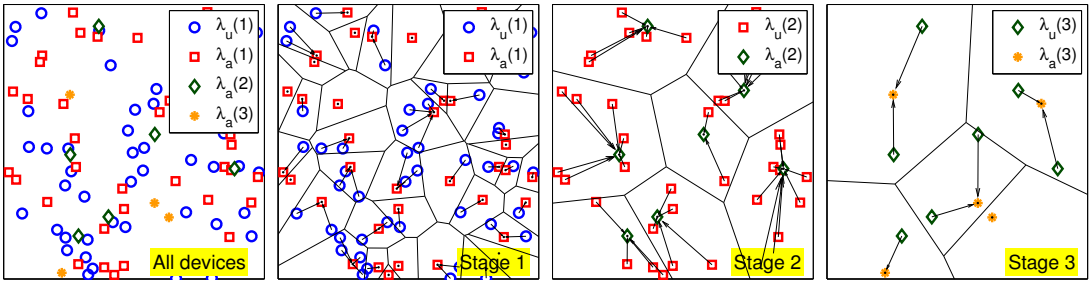

Fig. 1: A three-stage aggregation scheme with PPP($\lambda = 1$) device process. The aggregator processes (stage 1: $\square$, stage 2: $\diamondsuit$, stage 3: $*$) are obtained by thinning the original PPP, and have densities $\lambda_a(k) = 0.4^k$ for stages k=1:3. Density for the initial transmitter process (stage 1: $\circ$) is $\lambda_u(1) = \lambda - \sum_{k=1}^{3} \lambda_a(k)$, and for the transmitter processes for later stages are $\lambda_u(k) = \lambda_a(k-1)$ for $k > 2$, respectively. Last stage aggregators correspond to the BSs.

Proof. See Appendix A. $\square$

Corollary 1. *For no maximum power constraint, with open loop power control and with minimum average path loss association, the uplink SIR coverage is [13]*

$$\lim_{P_{T_{\max}} \to \infty} \mathcal{P}(T) \approx \exp\Big(- \frac{2T}{\alpha - 2} C_\alpha(T) \Big). \tag{5}$$

A. Coverage Probability and Number of Stages

The number of multi-hop stages K is mainly determined by the SIR coverage and the *distance coverage*, which we define as the probability that the distance between a device and its nearest aggregator is below a threshold. We provide bounds on K using these coverage concepts.

Assumption 2. Interstage independence. *The proposed hierarchical aggregation model introduces dependence among the stages of multi-hop communication since each subsequent stage is generated by the thinning of the previous stage. For analytical tractability, we assume that the multi-hop stages are independent of each other. Hence, the transmission is successful if and only if all the individual stages are successful. The success probability over K stages is*

$$\mathcal{P}_{\text{cov}}(K) = \mathbb{P}(\text{SIR}_1 > T, \ldots, \text{SIR}_K > T) = \prod_{k=1}^{K} \mathcal{P}_k(T),$$

where $\mathcal{P}_k(T)$ denotes the coverage probability at stage k. With full channel inversion and minimum average path loss association, the uplink SIR coverage is independent of the infrastructure density as given in (5). For the case $P_{T_{\max}} \to \infty$, since $\mathcal{P}_k(T)$ in (5) is also independent of the device density, and only depends on the threshold T and path loss exponent α, is identical for all stages, and denoted by $\mathcal{P}(T)$.

Lemma 2. *For any maximum power constraint $P_{T_{\max}}$, given a minimum probability of coverage requirement $\mathcal{P}_{\text{cov}}(K) > 1-\varepsilon$ and an SIR threshold T, the number of stages is upper bounded by*

$$K_{\text{U}} = \left\lceil \frac{\log\left(1/(1-\varepsilon)\right)}{-\log(\max_k \mathcal{P}_k(T))} \right\rceil. \tag{6}$$

Proof. The upper bound is obtained by combining (3) with the condition $\mathcal{P}_{\text{cov}}(K) > 1-\varepsilon$ and using the relation $\mathcal{P}_{\text{cov}}(K) = \prod_{k=1}^{K} \mathcal{P}_k(T) \leq \max_k \mathcal{P}_k(T)^K$. $\square$

In addition to the SIR outage, since the devices are randomly deployed, any device will be in outage when its nearest aggregator is outside its transmission range. Thus, we aim to investigate the minimum number of required stages given a distance outage constraint. A lower bound on the optimal number of multi-hop stages is given by the following Lemma.

Lemma 3. *The number of stages is lower bounded by*

$$K_{\text{L}} = \left\lceil \mathbb{E}[L(\lambda_a)] \mathbb{E}\Big[\frac{1}{\text{N}_\text{a}}\Big] \Big(\frac{P_{R_{\min}}}{P_{T_{\max}}}\Big)^{\frac{1}{\alpha}} \right\rceil, \tag{7}$$

where $L(\lambda_a)$ denotes the total length of the connections, N_a is the random variable that denotes the number of devices in the Voronoi cell of a typical BS or aggregator, $P_{T_{\max}}$ is the maximum transmit power and $P_{R_{\min}}$ is the minimum detectable signal power at the receiver.

Proof. The proof follows from the mean additive characteristic associated with the typical cell of the access network model provided in [14, Ch. 4.5]. The mean total length of connections in the Voronoi cell of an aggregator equals

$$\mathbb{E}[L(\lambda_a)] = \lambda_u \int_{\mathbb{R}^2} \|x\| \, e^{-\lambda_a \pi \|x\|^2} \, \mathrm{d}x = \lambda_u \lambda_a^{-3/2}/2. \tag{8}$$

Given a maximum transmitter power constraint, $P_{T_{\max}}$ for each device, the maximum transmission range is given by $(P_{T_{\max}}/P_{R_{\min}})^{1/\alpha}$. Dividing $L(\lambda_a)$ by N_a and taking its expectation with respect to the distribution of N_a, we obtain the mean length of connections[2], and dividing this ratio by the maximum transmission range, we get the desired result. $\square$

IV. Transmission Rate Models

For an interference limited network, the rate of the typical device is $\text{Rate} = \frac{W}{\text{N}_\text{a}} \log(1 + \text{SIR})$, where W is the total bandwidth of the communication channel, and N_a is the load at the typical aggregator. The average number of devices served by the typical aggregator is $\mathbb{E}[\text{N}_\text{a}] = \lambda_u/\lambda_a$. Rate coverage is defined as rate exceeding a given threshold, i.e.,

$$\mathbb{P}(\text{Rate} > \rho) = \sum_{l=0}^{\infty} \mathbb{P}\left(\text{SIR} > T | \text{N}_\text{a} = l\right) \mathbb{P}_{\text{N}_\text{a}}(l), \tag{9}$$

where $T = 2^{\frac{\rho \text{N}_\text{a}}{W}} - 1$ and $\mathbb{P}_{\text{N}_\text{a}}(l)$ is the probability mass function (PMF) of N_a, and is given by the following Lemma.

Lemma 4. *The PMF of the number of devices served per aggregator of stage k, i.e., $\text{N}_\text{a}(k)$, is*

$$\mathbb{P}_{\text{N}_\text{a}(k)}(l) = \frac{3.5^{3.5} (\lambda_u(k)/\lambda_a(k))^l}{(3.5 + (\lambda_u(k)/\lambda_a(k)))^{3.5+l}} \frac{\Gamma(3.5+l)}{\Gamma(3.5)\Gamma(l+1)}, \tag{10}$$

[2]For tractability, we take expectation over a PPP first to find $\mathbb{E}[L(\lambda_a)]$, and then multiply it by $\mathbb{E}\Big[\frac{1}{\text{N}_\text{a}}\Big]$ assuming independence.

where $\lambda_u(k)$ and $\lambda_a(k)$ for $k \geq 1$ are given in Table I.

Proof. Normalized distribution function of Voronoi cell areas in 2D can be modeled by [15] as $f(y) = \frac{3.5^{3.5}}{\Gamma(3.5)} y^{\frac{5}{2}} e^{-\frac{7}{2}y}$. Using the densities of the transmitters and the aggregators of stage k, the probability generating function (PGF) of the stage k devices in the random area y is [16]

$$G_{\mathrm{N_a}(k)}(z) = \mathbb{E}[\exp\left((\lambda_u(k)/\lambda_a(k))y(z-1)\right)], \quad (11)$$

which is of a Poisson random variable $\mathrm{N_a}(k)$ with mean $(\lambda_u(k)/\lambda_a(k))y$. The PMF of $\mathrm{N_a}(k)$ can be recovered by taking derivatives of $G_{\mathrm{N_a}(k)}(z)$ as $\mathbb{P}_{\mathrm{N_a}(k)}(l) = G^{(l)}_{\mathrm{N_a}(k)}(0)/l!$. □

The key assumption in our analysis is that there is one active device per resource block in each Voronoi cell. Using (10) the probability of not finding any device in the Voronoi cell of the typical aggregator at stage k is

$$\mathbb{P}_{\mathrm{N_a}(k)}(0) = G_{\mathrm{N_a}(k)}(0) = 3.5^{3.5}(3.5 + \mathbb{E}[\mathrm{N_a}(k)])^{-3.5}. \quad (14)$$

Let $p_{\mathrm{th}}(k)$ be the probability that there is at least one device in the Voronoi cell of the typical aggregator in the k^{th} stage. Therefore, the interference field of stage k is thinned by $p_{\mathrm{th}}(k)$, and the effective density of the interfering devices at stage k is $p_{\mathrm{th}}(k)\lambda_u(k)$. Using (14), $p_{\mathrm{th}}(k) = 1 - 3.5^{3.5}(3.5 + \mathbb{E}[\mathrm{N_a}(k)])^{-3.5}$. From Table I, we can see that $p_{\mathrm{th}}(k)$ is the same for $1 < k < K$, and different for $k \in \{1, K\}$.

We consider two main transmission protocols, namely i) a successive transmission protocol where the stages are activated sequentially, i.e., a half-duplex sequential mode, and ii) a parallel transmission mode, which is either a full-duplex protocol where all stages are simultaneously active, or a half-duplex protocol with alternating active stages.

A. Rate Distribution for Successive Stages

In this mode, each transmission cycle consists of the stages operating in succession. This mode may provide lower resource utilization, but it has low interference since multiple stages are not active simultaneously. Let $\mathcal{K} = \{1, \ldots, K\}$ denote the set of stages and $\mathcal{R} = \{\mathrm{Rate}_1, \ldots, \mathrm{Rate}_K\}$ be the set of transmission rates at each stage. The transmission rate in successive mode is given by $\mathrm{R_S} = K^{-1} \min_{k \in \mathcal{K}} \mathrm{Rate}_k$.

Remark 1. Dependence of hierarchical levels. *The hierarchical levels are not independent from each other and hence, it is not tractable to analyze the joint rate distribution for successive stages. Instead, we define the rate outage as in (15) where transmission rates are assumed independent. Without tracking the path of the bits (payload) transmitted, we only consider if the hierarchical transmission process is successful. Transmission from a device is successful if its payload is delivered to the BS at the end of K stages.*

With the independence assumption in Remark 1, the rate coverage for successive stages is

$$\mathbb{P}(\mathrm{R_S} > \rho) \approx \prod_{k \in \mathcal{K}} \sum_{l=0}^{\infty} \mathcal{P}_k(2^{\frac{K\rho l}{W}} - 1)\mathbb{P}_{\mathrm{N_a(k)}}(l). \quad (15)$$

If we let $P_{T_{\max}} \to \infty$, $\mathcal{P}_k(2^{\frac{K\rho l}{W}} - 1)$ is simplified to

$$\lim_{P_{T_{\max}} \to \infty} \mathcal{P}_k(2^{\frac{K\rho l}{W}} - 1) \approx \exp\Big(- \frac{2^{\frac{K\rho l}{W}} - 1}{\frac{\alpha}{2} - 1} C_\alpha(2^{\frac{K\rho l}{W}} - 1)\Big).$$

B. Rate Distribution for Full-Duplex Parallel Stages

In full-duplex mode, transmissions are not interrupted during a transmission cycle unlike the sequential mode. All stages operate in parallel, the 1^{st} stage devices only transmit, and the rest of the devices both transmit and aggregate simultaneously, during all stages of the multi-hop transmission.

Due to the simultaneous transmissions at all levels of the hierarchical model, the interference at each stage is due to i) the interferers of that stage, i.e., the intra-stage interference, and ii) the remaining transmitting devices of the other stages, i.e., the inter-stage interference. The hierarchical levels are determined in the same manner similar to the successive mode, and also dependent in this mode, and hence, the inter-stage interference is correlated. Although full-duplex parallel mode offers high resource utilization compared to successive mode, it has higher interference since all the stages are active. The intra-stage interference in the parallel mode can be obtained in the similar manner as in the successive mode. Lemma 5 (See next page.) provides the analytical expressions for the Laplace transforms of intra-stage and inter-stage interference.

Corollary 2. *The Laplace transform of the total inter-stage interference for $P_{T_{\max}} \to \infty$ is*

$$\mathcal{L}_{I_{k^c}}(s) \approx \exp\Big(- B_\alpha(s\overline{P}_T) - \frac{2s\overline{P}_T}{\alpha - 2} C_\alpha(s\overline{P}_T)\Big)^{(K-1)}. \quad (16)$$

Lemma 6. *The uplink SIR coverage probability for the full-duplex parallel mode is given by*

$$\mathbb{P}(\mathrm{SIR_P} > T) \approx \prod\nolimits_{k \in \mathcal{K}} \Big(p_k \mathcal{L}_{I_k}(T\overline{P}_T^{-1}) \mathcal{L}_{I_{k^c}}(T\overline{P}_T^{-1}) + \int_{r_c}^{\infty} \mathcal{L}_{I_k}(Tr^\alpha P_{T_{\max}}^{-1}) \mathcal{L}_{I_{k^c}}(Tr^\alpha P_{T_{\max}}^{-1}) f_{R_k}(r)\, \mathrm{d}r \Big), \quad (17)$$

where $f_{R_k}(r) = (r/\sigma_k^2) e^{-r^2/2\sigma_k^2}$ for $\sigma_k = \sqrt{1/(2\pi\lambda_a(k))}$.

Proof. The proof is similar to that of Theorem I in [13]. However, instead of one serving stage, the serving stages change sequentially. Result follows from the evaluation of (12) using (3). Since the total inter-stage interference in (13) is independent from the intra-stage interference, its Laplace transform is incorporated as a multiplicative term. □

Lemma 7. *Letting $T_l = 2^{\frac{\rho l}{W}} - 1$, the rate coverage probability for the full-duplex parallel transmission mode is given by*

$$\mathbb{P}(\mathrm{R_P} > \rho) = \prod_{k \in \mathcal{K}} \sum_{l=0}^{\infty} \mathbb{P}(\mathrm{SIR}_k > T_l | \mathrm{N_a}(k) = l) \mathbb{P}_{\mathrm{N_a(k)}}(l). \quad (18)$$

Remark 2. *The models described above, i.e., the sequential mode which is half-duplex by design, and the full-duplex parallel mode, are the two principle design schemes that mainly differ in terms of their total rate coverages. Although the full-duplex strategy is probably not feasible for M2M communication, it is helpful to have a comparison of the rate distributions of both models, and provided for completeness.*

Next, we introduce the half-duplex parallel transmission.

C. Rate Distribution for Half-Duplex Parallel Stages

The full-duplex parallel mode can be transformed into a half-duplex communication scheme. In this mode, at a

Lemma 5. *The Laplace transforms of the intra-stage interference and the inter-stage interference are given as follows:*
(a) The Laplace transform of the intra-stage interference at stage k is

$$\mathcal{L}_{I_k}(s) \approx \exp\Big(- \frac{2s}{\alpha-2}\Big((1-e^{-\pi\lambda_a^{\text{eff}}(k)r_c^2}(1+\pi\lambda_a^{\text{eff}}(k)r_c^2))\overline{P}_T C_\alpha(s\overline{P}_T) + (1-p_k)\pi\lambda_a^{\text{eff}}(k)P_{T_{\max}}\mathbb{E}_{R_{z_k}}\Big[R_{z_k}^{2-\alpha}C_\alpha\Big(\frac{sP_{T_{\max}}}{R_{z_k}^\alpha}\Big)\Big|R_{z_k}>r_c\Big]\Big)\Big), \quad (12)$$

where $p_k = 1-\exp(-\pi\lambda_a(k)r_c^2)$ and $\lambda_a^{\text{eff}}(k) = p_{\text{th}}(k)\lambda_a(k)$.
(b) The Laplace transform of the total inter-stage interference from stages $\{l|\, l\in\mathcal{K}, l\neq k\}$ is

$$\mathcal{L}_{I_{k^c}}(s) \approx \prod\nolimits_{l\in k^c}\exp\Big(- (1-e^{-\pi\lambda_a^{\text{eff}}(l)r_c^2}(1+\pi\lambda_a^{\text{eff}}(l)r_c^2))(B_\alpha(s\overline{P}_T) + \frac{2s\overline{P}_T}{\alpha-2}C_\alpha(s\overline{P}_T)) - (1-p_l)\pi\lambda_a^{\text{eff}}(l)\mathbb{E}_{R_{z_l}}\Big[R_{z_l}^2\Big(B_\alpha\Big(\frac{sP_{T_{\max}}}{R_{z_l}^\alpha}\Big) + \frac{2sP_{T_{\max}}}{(\alpha-2)R_{z_l}^\alpha}C_\alpha\Big(\frac{sP_{T_{\max}}}{R_{z_l}^\alpha}\Big)\Big)\Big|\, R_{z_l}>r_c\Big]\Big), \quad (13)$$

where $B_\alpha(s) = {}_2F_1\big(1,\frac{2}{\alpha},1+\frac{2}{\alpha},-\frac{1}{s}\big)$ is obtained using the Gauss-Hypergeometric function.

Proof. Proof is skipped due to space constraints. It is provided in the extended version of this paper [17]. □

particular time slot, only the even or odd stages are active. Analysis of this model is quite similar to the parallel mode analysis, using only the active stages when calculating the inter-stage interference. The SIR coverage of the half-duplex mode can be characterized by the following lemma.

Lemma 8. *The uplink SIR coverage probability for the half-duplex parallel mode is given by*

$$\mathbb{P}(\text{SIR}_{\text{P}} > T) \approx \prod\nolimits_{k\in\mathcal{K}_{\text{H}}}\Big(p_k\mathcal{L}_{I_k}(T\overline{P}_T^{-1})\mathcal{L}_{I_{k^c}}(T\overline{P}_T^{-1}) + \int_{r_c}^{\infty}\mathcal{L}_{I_k}(Tr^\alpha P_{T_{\max}}^{-1})\mathcal{L}_{I_{k^c}}(Tr^\alpha P_{T_{\max}}^{-1})f_{R_k}(r)\,\mathrm{d}r\Big). \quad (19)$$

where calculations of $\lambda_a^{\text{eff}}(k)$ and the distributions of $\{R_{z_k}\}$ in (12)-(13) are done over the set of active stages and $\mathcal{K}_{\text{H}}$ denotes the set of active stages, i.e., the even or the odd stages.

For the half-duplex mode, the rate coverage expression in (18) changes in accordance with (19), which can be found by following the steps in Lemma 7. Since only half of the stages are active simultaneously, the overall rate is half the rate of the active stages. Thus, to achieve a rate threshold of ρ, the rate threshold for the active stages should be set to 2ρ.

V. Numerical Results

The simulation setup for the verification of analytical rate models developed in Sect. IV is as follows. Device locations are distributed as PPP over a square region of size 5×5 sq. km. Total bandwidth is $W = 10^5$Hz, $\alpha = 4$, device and BS densities are $\lambda = 10^3$ and $\lambda_{\text{BS}} = 1$ per sq. km., and the device payload is $M = 100$ bits. Note that the density of aggregators at stage k is $\lambda\gamma^k$, i.e., the number of aggregators decay geometrically. Therefore, for high K values we need a region with much larger area for the validation of the model, but scaling the region increases the computational complexity exponentially. Therefore, we restrict ourselves to $K = 1:3$, and investigate the performance of the proposed model.

The rate coverages for the sequential and the full-duplex modes are illustrated in Figs. 2 and 3. The results provide tight approximation despite the *interstage independence assumption* in Sect. III-A, and the *independent power control assumption* in [12]. The full-duplex mode does not offer higher rate coverage compared to sequential mode, which is due to *inter-stage interference* as detailed in Sect. IV-B. Thus, in terms of rate coverage, sequential mode is preferable over full-duplex mode. Furthermore, the half-duplex parallel mode has higher coverage than full-duplex mode for the same K. Due to limited space, we do not provide an illustration for that scheme.

Considering the operating regime for M2M devices and their design simplicity, sequential and half-duplex parallel modes are feasible techniques and preferable as they have high coverage. Different transmission modes also have different energy demands. Investigation of the coverage and the energy requirements for these schemes can reveal the tradeoffs further, which is provided in the extended version of this paper [17].

Based on the numerical results, the take-away message is that devices should not do aggregation, i.e., direct transmission provides the highest rate. However, this is true if we assume the fraction of aggregators, i.e., γ, is kept fixed for any number of stages. One of the reasons for multi-hop transmissions is the distance constraint between the device and aggregator. If the devices are restricted to transmit over shorter distances to compensate the transmit power constraint, then γ should increase, which shifts their rate coverage curves towards right. Although our aggregation model is SIR-based, including noise is a natural way to limit the link distances and decrease the coverage. Therefore, noise will not have a strong influence on the analysis and our conclusions will not be effected much.

VI. Conclusions

We study a general multi-hop-based uplink communication scheme for M2M communication, and develop SIR and rate coverage models for M2M devices for different transmission schemes, using tools from stochastic geometry. Considering the operating regime of interest for M2M devices, sequential and half-duplex parallel modes are more feasible compared to full-duplex mode. Interesting extensions would include the minimization of the energy expenditure through joint optimization of the optimal number of multi-hop stages and fraction of aggregators. Strategies for synchronization of transmissions is also important to prevent multi-hop delays and save energy.

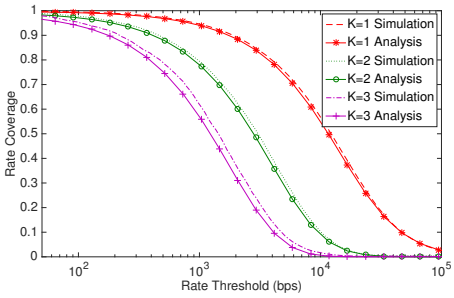

Fig. 2: Rate coverage for sequential mode, $K = \{1, 2, 3\}$.

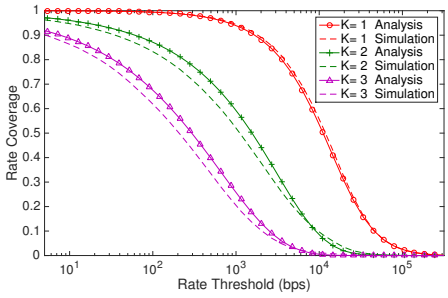

Fig. 3: Rate coverage for full-duplex mode, $K = \{1, 2, 3\}$.

APPENDIX

A. Proof of Lemma 1

The Laplace transform of the interference can be written as

$$\mathcal{L}_{I_r}(s) \overset{(a)}{=} \mathbb{E} \prod_{z \in \Psi_u \setminus \{x\}} \mathbb{E}_{R_z}\left[\frac{1}{1 + s \min\{P_{T_{\max}}, \overline{P}_T R_z^{\alpha}\} D_z^{-\alpha}}\right]$$

$$\overset{(b)}{\approx} e^{-\int_{y>0}\left(1-\mathbb{E}_{R_z}\left[\frac{1}{1+s\min\{P_{T_{\max}}, \overline{P}_T R_z^{\alpha}\} y^{-\alpha}} \middle| R_z < y\right]\right)\Lambda_u(\mathrm{d}y)}$$

$$\overset{(c)}{=} e^{-\int_{y>0} p \mathbb{E}_{R_z}\left[\frac{1}{1+s^{-1}\overline{P}_T^{-1} R_z^{-\alpha} y^{\alpha}} \middle| R_z < y, R_z < r_c\right]\Lambda_u(\mathrm{d}y)}$$

$$e^{-\int_{y>0}(1-p)\mathbb{E}_{R_z}\left[\frac{1}{1+s^{-1}P_{T_{\max}}^{-1} y^{\alpha}} \middle| R_z < y, R_z > r_c\right]\Lambda_u(\mathrm{d}y)}$$

$$\overset{(d)}{=} e^{-\pi\lambda_a p \mathbb{E}_{R_z}\left[R_z^2 \int_1^{\infty} \frac{1}{1+s^{-1}\overline{P}_T^{-1} t^{\alpha/2}} \mathrm{d}t \middle| R_z < r_c\right]}$$

$$e^{-\pi\lambda_a (1-p)\mathbb{E}_{R_z}\left[\int_1^{\infty} R_z^2 \frac{1}{1+s^{-1}P_{T_{\max}}^{-1} t^{\alpha/2} R_z^{\alpha}} \mathrm{d}t \middle| R_z > r_c\right]}$$

$$\overset{(e)}{=} e^{-\pi\lambda_a p \mathbb{E}_{R_z}\left[R_z^2 | R_z < r_c\right]\frac{2}{\alpha-2} s \overline{P}_T C_{\alpha}(s\overline{P}_T)}$$

$$e^{-\pi\lambda_a (1-p)\mathbb{E}_{R_z}\left[R_z^2 \frac{2}{\alpha-2} s P_{T_{\max}} R_z^{-\alpha} C_{\alpha}(s P_{T_{\max}} R_z^{-\alpha}) \middle| R_z > r_c\right]}$$

$$\overset{(f)}{=} e^{-\frac{2s}{\alpha-2}(1-e^{-\pi\lambda_a r_c^2}(1+\pi\lambda_a r_c^2))\overline{P}_T C_{\alpha}(s\overline{P}_T)}$$

$$e^{-\frac{2s}{\alpha-2}(1-p)\pi\lambda_a P_{T_{\max}} \mathbb{E}_{R_z}\left[R_z^{2-\alpha} C_{\alpha}(s P_{T_{\max}} R_z^{-\alpha}) \middle| R_z > r_c\right]},$$

where (a) follows from the iid nature of $\{g_z\}$ and the independence of $\{R_z\}$ (see Assumption 1). The process Ψ_u is not a PPP but a Poisson-Voronoi perturbed lattice and hence the functional form of the interference (or the Laplace functional of Ψ_u) is not tractable [13]. Authors in [13] propose an approximation to characterize the corresponding process as an inhomogeneous PPP with intensity measure function $\Lambda_u(\mathrm{d}y) = 2\pi\lambda_a y(\mathrm{d}y)$. Hence, (b) follows from the definition of probability generating functional (PGFL) of the PPP [18], and the independent path loss between the device and its serving aggregator [13], i.e., R_z^{α}'s are independent, (c) follows from the maximum power constraint, where $p = 1 - \exp\left(-\pi\lambda_a r_c^2\right)$ denotes the probability that $R_z < r_c$, (d) follows from change of variables $t = (y/R_z)^2$, (e) follows using the definition of Gauss-Hypergeometric function, yielding $\int_1^{\infty} \frac{1}{1+s^{-1}t^{\alpha/2}} \mathrm{d}t = \frac{2s}{\alpha-2} {}_2F_1\left(1, 1-\frac{2}{\alpha}, 2-\frac{2}{\alpha}, -s\right) = \frac{2s}{\alpha-2} C_{\alpha}(s)$, (f) follows from Assumption 1 for R_z. Hence, R_z^2 is exponentially distributed with rate parameter $1/(2\sigma^2) = \pi\lambda_a$ that yields $p\mathbb{E}_{R_z}\left[R_z^2 | R_z < r_c\right] = \frac{1-e^{-\pi\lambda_a r_c^2}(1+\pi\lambda_a r_c^2)}{\pi\lambda_a}$.

Conditioned on the distance between the device and its associated aggregator, $\mathbb{P}(\mathrm{SIR} > T | r < r_c) = \mathbb{E}_{I_r}\left[\mathbb{P}\left(g > T\overline{P}_T^{-1} I_r | r < r_c\right)\right] \approx \mathcal{L}_{I_r}(T\overline{P}_T^{-1})$, and $\mathbb{P}(\mathrm{SIR} > T | r > r_c) = \mathbb{E}_{I_r}\left[\mathbb{P}\left(g > T r^{\alpha} P_{T_{\max}}^{-1} I_r | r > r_c\right)\right] \approx \mathcal{L}_{I_r}(T r^{\alpha} P_{T_{\max}}^{-1})$. Hence, the uplink SIR coverage is obtained as $\mathcal{P}(T) \approx p\mathcal{L}_{I_r}(T\overline{P}_T^{-1}) + \int_{r_c}^{\infty} \mathcal{L}_{I_r}(T r^{\alpha} P_{T_{\max}}^{-1}) f_R(r)\,\mathrm{d}r$, where $R \sim$Rayleigh(σ) with $\sigma = \sqrt{1/(2\pi\lambda_a)}$.

REFERENCES

[1] "Cisco visual networking index: Global mobile data traffic forecast update, 2014-2019," white paper, Cisco, Feb. 2015.

[2] H. S. Dhillon, H. Huang, and H. Viswanathan, "Wide-area wireless communication challenges for the Internet of Things," *submitted, arXiv preprint arXiv:1504.03242*, 2015.

[3] H. S. Dhillon, H. C. Huang, H. Viswanathan, and R. A. Valenzuela, "Power-efficient system design for cellular-based machine-to-machine communications," *IEEE Trans. Wireless Commun.*, vol. 12, no. 11, pp. 5740–5753, Nov. 2013.

[4] ——, "Fundamentals of throughput maximization with random arrivals for M2M communications," *IEEE Trans. Commun.*, vol. 62, no. 11, pp. 4094–4109, Nov. 2014.

[5] A. Aijaz, M. Tshangini, M. Nakhai, X. Chu, and H. Aghvami, "Energy-efficient uplink resource allocation in LTE networks with M2M/H2H co-existence under statistical QoS guarantees," *IEEE Trans. Commun.*, vol. 62, pp. 2353–2365, 2014.

[6] S. Bandyopadhyay and E. J. Coyle, "An energy efficient hierarchical clustering algorithm for wireless sensor networks." in *Proc., IEEE Infocom*, vol. 3, Apr. 2003, pp. 1713–1723.

[7] V. Rodoplu and T. Meng, "Minimum energy mobile wireless networks," *IEEE J. Sel. Areas Commun.*, vol. 17, 1999.

[8] F. Baccelli and S. Zuyev, "Poisson-Voronoi spanning trees with applications to the optimization of communication networks," *Operations Research*, vol. 47, no. 4, pp. 619–631, 1999.

[9] S. J. Baek, G. de Veciana, and X. Su, "Minimizing energy consumption in large-scale sensor networks through distributed data compression and hierarchical aggregation," *IEEE J. Sel. Areas Commun.*, vol. 22, no. 6, pp. 1130–1140, Aug. 2004.

[10] M. Haenggi and D. Puccinelli, "Routing in ad hoc networks: A case for long hops," *IEEE Commun. Mag.*, vol. 43, 2005.

[11] A. Laya, L. Alonso, and J. Alonso-Zarate, "Is the random access channel of LTE and LTE-A suitable for M2M communications? A survey of alternatives," *IEEE Commun. Surveys Tuts.*, vol. 16, pp. 1–13, 2014.

[12] T. D. Novlan, H. S. Dhillon, and J. G. Andrews, "Analytical modeling of uplink cellular networks," *IEEE Trans. Wireless Commun.*, vol. 12, no. 6, pp. 2669–2679, Jun. 2013.

[13] S. Singh, X. Zhang, and J. G. Andrews, "Joint rate and SINR coverage analysis for decoupled uplink-downlink biased cell associations in HetNets," *IEEE Trans. Wireless Commun.*, vol. 14, no. 10, Oct. 2015.

[14] F. Baccelli and B. Błaszczyszyn, *Stochastic Geometry and Wireless Networks, Volume I — Theory*, ser. Foundations and Trends in Networking. NoW Publishers, 2009, vol. 3, no. 3–4.

[15] J.-S. Ferenc and Z. Neda, "On the size-distribution of Poisson Voronoi cells," *Physica A: Statistical Mechanics and its Applications*, vol. 385, no. 2, Nov. 2007.

[16] S. Singh, H. Dhillon, and J. Andrews, "Offloading in heterogeneous networks: Modeling, analysis, and design insights," *IEEE Trans. Wireless Commun.*, vol. 12, no. 5, pp. 2484–2497, 2013.

[17] D. Malak, H. S. Dhillon, and J. G. Andrews, "Optimizing data aggregation for uplink machine-to-machine communication networks," *to appear, IEEE Trans. Commun., arXiv preprint arXiv:1505.00810v2*, 2016.

[18] D. Stoyan, W. Kendall, and J. Mecke, *Stochastic Geometry and Its Applications*, 2nd ed. John Wiley and Sons, 1996.